# Structural transition of $Li_2BeH_4$ under high pressure: A first-principles study

C. H. Hu,[1] D. M. Chen,[1] Y. M. Wang,[2,*] D. S. Xu,[2] and K. Yang[1]

[1]*National Engineering Research Center, Institute of Metal Research, Chinese Academy of Sciences, 72 Wenhua Road, Shenyang 110016, People's Republic of China*

[2]*Shenyang National Laboratory for Materials Science, Institute of Metal Research, Chinese Academy of Sciences, 72 Wenhua Road, Shenyang 110016, People's Republic of China*

(Received 29 September 2006; revised manuscript received 23 January 2007; published 13 June 2007)

We present a systematic first-principles investigation of the high-pressure structural stability of $Li_2BeH_4$. Our total-energy calculations show that at ambient pressure, the structure of $\alpha$-$Li_2BeH_4$ observed in experiments is more stable than the other proposed structures in this work and the structural transformation from $\alpha$ to $\beta$ ($Cs_2MgH_4$ type; *Pnma*) occurs at 18.1 GPa, together with a volume reduction of 4.7%. A detailed study of their electronic structures under ambient pressure up to 30.0 GPa reveals that this behavior is closely related to the variation in the Be–H covalent bonding in the $BeH_4$ anionic subunits of $Li_2BeH_4$. Based on a colligated analysis of the covalent bond number per unit area ($N_a$) and the scaled bond overlap population ($BOP^s$), $\beta$-$NaAlH_4$ and $\beta$-$Mg(AlH_4)_2$ are expected to be the most promising candidates for hydrogen storage among the other investigated materials. However, the improvement of hydrogen absorption and/or desorption for $Li_2BeH_4$ is less significant.

DOI: 10.1103/PhysRevB.75.224108 PACS number(s): 31.15.Ew, 68.18.Jk

## I. INTRODUCTION

Exploring a safe, cost-effective, and fully hydrogenation-reversible hydrogen storage material with a higher gravimetric hydrogen density (GHD) in excess of 6.5 wt % is one of the targets for developing next-generation energy storage systems.[1,2] It had been difficult for conventional hydrides such as $LaNi_5$-H and $TiFe_{1.8}$-H, and Laves phase systems to satisfy the requirement of a high GHD, although they have good cycling performance under ambient conditions. The complex hydrides are generally thought to be the most promising candidates because of their high GHD.[3–7] For example, sodium alanate, $NaAlH_4$, and magnesium alanate, $Mg(AlH_4)_2$, have 7.5 and 9.6 wt % theoretical hydrogen capacities, respectively. Unfortunately, these hydrides have been considered to be intrinsically noncyclable energy storage materials due to their high desorption temperatures for a long time. Recently, they have attracted attention because Bogdanovic and Schnickardi[3] found that $NaAlH_4$ can rapidly release 5.6 wt % H at moderate temperatures by adding transition-metal catalysts.

Apart from the two known hydrides, $BeH_2$ and $LiBH_4$, having higher hydrogen capacities (18.3 and 18.5 wt %, respectively), lithium beryllium hydride, $Li_2BeH_4$, is also a good candidate for hydrogen storage due to its high GHD (15.0 wt %). Although Bell and Coates[8] were the first to synthesize experimentally the $Li_2BeH_4$ compound, they failed to determine its crystal structure. Based on a new interpretation of the powder-diffraction data given by Bell and Coates, Bastide[9] further determined that $Li_2BeH_4$ has a monoclinic distorted perovskite-type structure. However, more crystallographic information on atomic positions was not given. Recently, Bulychev *et al.*[10] characterized successfully its structure by means of x-ray and neutron powder-diffraction techniques. Shortly after, Lipinska-Kalita *et al.*[11] investigated its high-pressure behavior by a synchrotron-radiation technique based on x-ray diffraction and high-pressure Raman spectroscopy and declared that in the range from 10 to 20 GPa, the pressure-induced structural transformations would occur with increasing pressure. A more detailed structural information, however, was not given in their work. Although some researchers described theoretically the ground-state electronic structure of $LiBeH_3$ with a hypothetical crystal structure using first-principles methods,[12–15] to our best knowledge, a systematic study on the electronic structure of $Li_2BeH_4$ has not been reported yet. In addition, as mentioned in the paper of Bulychev *et al.*[10] it was difficult to determine the precise positions of atoms with a low atomic number due to their poor scattering ability to neutrons in these compounds. It is much more difficult to describe their high-pressure behavior, governed by the intermolecular as well as intermolecular interactions, by experiments only, without the help of theoretical calculations.

In fact, first-principles methods have been successfully applied to predict the pressure-induced structural transition of $MgH_2$,[16] $LiAlH_4$,[17] $NaAlH_4$,[18] and $NaBH_4$,[19] in which their phase transitions have also been reproduced by high-pressure experiments.[19–22] Our first-principles total-energy calculations for the pressure-induced phase transitions in the $Mg(AlH_4)_2$ system have been completed,[23] in which we predicted that with compressing the volume, the two structural transitions take place from a prototype $\alpha$ structure to a $\beta$ structure [$\delta$-$Zr(MoO_4)_2$ type], and then to a $\gamma$ structure [$Ca(BF_4)_2$ type] at 0.67 and 10.3 GPa, respectively. The above success makes us confident that the density-functional theory (DFT) approach is a powerful tool for investigating the phase transitions of such materials and could provide some useful information for experiments. The main aim of the present work is to study the phase transitions of $Li_2BeH_4$ under high-pressure conditions using first-principles calculations.

The paper is organized as follows: First, computational details are described in Sec. II. Then, in Sec. III, we present the detailed calculation results and then discuss the intrinsic

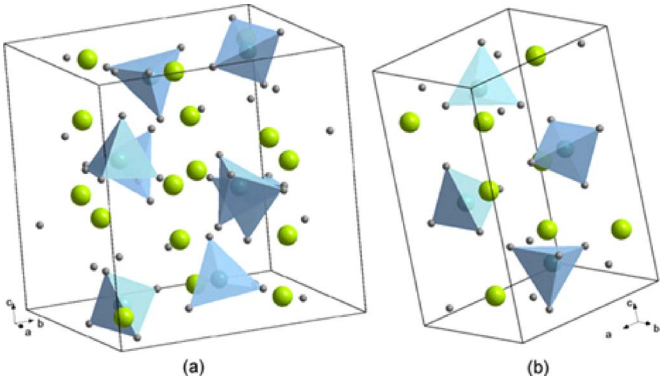


FIG. 1. (Color online) Crystal structure of (a) $\alpha$-$Li_2BeH_4$ (monoclinic; $P2_1/c$) and (b) $\beta$-$Li_2BeH_4$ ($Cs_2MgH_4$ type; orthorhombic; *Pnma*). The tetrahedra represent $BeH_4$ subunits, where the Be atom is located in the center and the four H atoms at the vertices of each.

relations between the mechanical properties and electronic structures in $Li_2BeH_4$. Finally, the conclusions are summarized in Sec. IV.

## II. COMPUTATIONAL DETAILS

All the electronic structure calculations in this work were performed within DFT, using the PW91 generalized gradient approximation (GGA) functional.[24] A plane-wave ultrasoft pseudopotential method as implemented in the CASTEP code[25] was employed. The geometric optimization of a computational cell was carried out with the BFGS minimization algorithm[26] provided in this code. The main advantage of the BFGS is that cell optimizations in the mixed space of both internal and cell degrees of freedom, including the optimization at fixed external stress, can be performed. The Pulay density mixing scheme[27] was used to generate a new starting charge density during the self-consistent-field (SCF) total-energy calculations. The SCF calculations were converged when the energy threshold was lower than $10^{-6}$ eV/atom. In order to decrease the error resulting from the choice of the plane-wave basis sets and $k$ points, as well as to guarantee comparable computational precision, the cut-off energy was set to 300 eV in all calculations. Moreover, a $k$-point spacing smaller than 0.03 $Å^{-1}$ was individually adjusted in reciprocal space, not only to the size of each computational cell of the nine crystallographic structures of $Li_2BeH_4$ given below but also to its variation at a given compressed volume.

## III. RESULTS AND DISCUSSION

Recent x-ray powder-diffraction experiments[10] have established the structure of $\alpha$-$Li_2BeH_4$, shown in Fig. 1(a), in which $BeH_4$ forms an almost regular tetrahedral subunit with the Be atom at its center and four H atoms at its vertices, and Li atoms are located in the interstices of the structure composed of those $BeH_4$ subunits. In our total-energy calculations, the nine closely related potential crystallographic structures are considered. They are, namely, $\alpha$-$Li_2BeH_4$ (monoclinic; $P2_1/c$),[10] $Cs_2MgH_4$ (orthorhombic; *Pnma*),[28]

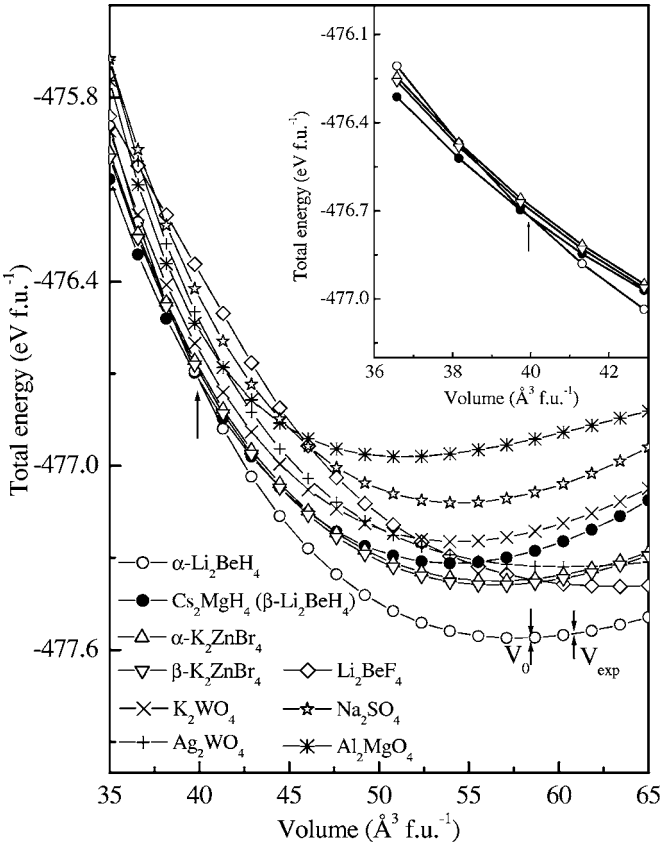


FIG. 2. Total energy (in eV $f.u.^{-1}$) versus the atomic volume (in $Å^3$ $f.u.^{-1}$) for $\alpha$-$Li_2BeH_4$ and other proposed structures. For clarity, the part near the transition point is enlarged and shown in the inset. The experimental volume ($V_{expt}$=61.315 $Å^3$ $f.u.^{-1}$) and optimized equilibrium volume ($V_0$=57.658 $Å^3$ $f.u.^{-1}$) for $\alpha$-$Li_2BeH_4$ are marked by the inverse arrows. The $\alpha \rightarrow \beta$ structural transition point is indicated by an arrow.

$Li_2BeF_4$ (trigonal; $R$-3),[29] $Na_2SO_4$ (trigonal; $P$-3$m$1),[30] $K_2WO_4$ (monoclinic; $C2/m$),[31] $Ag_2WO_4$ (orthorhombic; $Pnn2$),[32] $Al_2MgO_4$ (cubic; $Fd$-3$m$),[33] $\alpha$-$K_2ZnBr_4$ (monoclinic; $P2_1/m$),[34] and $\beta$-$K_2ZnBr_4$ (monoclinic; $P2_1$).[34]

In order to show how the structure of $Li_2BeH_4$ varies under pressure, for each proposed structure, the equilibrium geometry and zero-temperature Gibbs free energy (total energy plus $PV$ or enthalpy) at more than nine pressure points in the range from 0 to 30.0 GPa are obtained by the complete optimization of the structural parameters, as mentioned above. The calculated total energy (Gibbs free energy minus $PV$) versus the compressed volume ($E$-$V$) curves for 1 f.u. of these proposed structures are obtained by fitting the Vinet equation of state (V-EOS),[35] the Murnaghan EOS,[36] and the Birch EOS,[37] respectively. There is no significant difference in these curves. But the curves from V-EOS are in better agreement with the experimental data in the high-pressure range.[35] Thus, in this paper, we restrict ourselves to the V-EOS results, as shown in Fig. 2. Figure 2 evaluates the energy and stability of each of the proposed structures. It can be found from this figure that at ambient conditions, $\alpha$-$Li_2BeH_4$ with the lowest energy is more stable than the other structures considered in the present study. Furthermore,

TABLE I. Optimized structural parameters: Lattice constants (in Å), internal atomic positions (in fractional coordinates), bulk modulus $B_0$ (in GPa), and its pressure derivative $B_0'$ for $\alpha$-$Li_2BeH_4$ and $\beta$-$Li_2BeH_4$ ($Cs_2MgH_4$ type). For comparison, the experimental values of $\alpha$-$Li_2BeH_4$ are given in parentheses.

| Structure | Lattice constants (Å) | Internal atomic positions | $B_0$ (GPa) | $B_0'$ |
|---|---|---|---|---|
| $\alpha$-$Li_2BeH_4$ | $a$=7.017 (7.062) | Li1: 0.6827, 0.0745, 0.4450 (0.6879, 0.0777, 0.4405) | 28.4 | 3.21 |
| ($P2_1/c$) | $b$=8.178 (8.338) | Li2: 0.1109, 0.2152, 0.4171 (0.1219, 0.2136, 0.4176) | | |
| | $c$=8.259 (8.347) | Li3: 0.8306, 0.0855, 0.0943 (0.8461, 0.0776, 0.0923) | | |
| | $\beta$=93.593 (93.577) | Li4: 0.4119, 0.9318, 0.2080 (0.4128, 0.9263, 0.2073) | | |
| | | Be1: 0.9641, 0.0690, 0.6992 (0.9652, 0.0681, 0.7018) | | |
| | | Be2: 0.4831, 0.2072, 0.0640 (0.4859, 0.2090, 0.0630) | | |
| | | H1: 0.2155, 0.0029, 0.3505 (0.2122, 0.0046, 0.3508) | | |
| | | H2: 0.9701, 0.0918, 0.8715 (0.9714, 0.0947, 0.8671) | | |
| | | H3: 0.6437, 0.2009, 0.9660 (0.6432, 0.2002, 0.9656) | | |
| | | H4: 0.4556, 0.1223, 0.5926 (0.4379, 0.1277, 0.5920) | | |
| | | H5: 0.0020, 0.2183, 0.6191 (0.0018, 0.2137, 0.6197) | | |
| | | H6: 0.5453, 0.1281, 0.2118 (0.5421, 0.1331, 0.2102) | | |
| | | H7: 0.8978, 0.0542, 0.3270 (0.9030, 0.0585, 0.3311) | | |
| | | H8: 0.3233, 0.1317, 0.9806 (0.3326, 0.1255, 0.9808) | | |
| $\beta$-$Li_2BeH_4$ | $a$=5.642 | Li1: 0.1401, 0.2500, 0.4538 | 37.2 | 2.41 |
| ($Pnma$) | $b$=4.691 | Li2: 0.4802, 0.2500, 0.6899 | | |
| | $c$=8.372 | Be: 0.2110, 0.2500, 0.0700 | | |
| | | H1: 0.7940, 0.2500, 0.5916 | | |
| | | H2: –0.0345, 0.2500, 0.0773 | | |
| | | H3: 0.3146, 0.0034, 0.1423 | | |

among all $E$-$V$ curves, the curves for the $\alpha$-$Li_2BeH_4$- and $Cs_2MgH_4$-type structures depicted in Fig. 1(b) (hereafter $\beta$-$Li_2BeH_4$) intersect at a volume of 39.8 Å$^3$, as marked by the arrow in Fig. 2. This implies that the structural transition would be from the $\alpha$- to the $\beta$-$Li_2BeH_4$ ($\alpha \rightarrow \beta$). With further compression of the volume, however, no other point of intersection with the $E$-$V$ curve for the $\beta$ phase is found, demonstrating that only one phase transition occurs at a certain pressure, in agreement with the previous report given by Lipinska-Kalita *et al.*[11] The optimized lattice parameters and atomic coordinates of $\alpha$- and $\beta$-$Li_2BeH_4$ are compiled in Table I. As shown in this table, for $\alpha$-$Li_2BeH_4$, the deviations between our calculated results and the experimental findings for the lattice constants and the internal parameters are not larger than 2%, which means that our calculations are reliable. By fitting the $E$-$V$ curves for $\alpha$- and $\beta$-$Li_2BeH_4$ using the V-EOS, their bulk moduli $B_0$ and corresponding pressure derivatives $B_0'$ are listed in the same table. Unfortunately, to the best of our knowledge, the experimental values for these are not yet available for comparison. Although $\beta$-$Li_2BeH_4$ is theoretically a harder phase than $\alpha$-$Li_2BeH_4$, for which the main reason is that $\beta$ has a lower equilibrium volume than $\alpha$, it is still an easily compressible material compared with classical hydrides, for example, the $B_0$ values of $MgH_2$,[16] $TiH_2$,[38] and $LaNi_5H_7$ (Ref. 39) are 51.0, 135.3, and 140.0 GPa, respectively.

Although the phase-transition pressure $P_T$ can be deduced from the common tangent between the total energy versus volume curves corresponding to the $\alpha$- and $\beta$-$Li_2BeH_4$ phases, it can be reliably and readily obtained by evaluating the enthalpy as a function of pressure for $\alpha$- and $\beta$-$Li_2BeH_4$. In order to give a clear picture of the $P_T$, the calculated curve of enthalpy difference ($H_\beta - H_\alpha$) versus pressure ($P$), together with the volume-pressure ($V$-$P$) curve, is obtained using the V-EOS, as shown in Fig. 3. In this figure, $H_\beta - H_\alpha$ becomes negative once the external pressure is beyond 18.1 GPa, at which the transition pressure ($P_T$) from the $\alpha$ to the $\beta$ phase is established and also comparable to the experimental results between 10 and 20 GPa given in the report of Lipinska-Kalita *et al.*[11] At this pressure, the corresponding volume reduction $\Delta V/V$ is about 4.7%, as marked in the $V$-$P$ curve. Such a large volume reduction at a transition point has been indeed observed in many high-pressure x-ray powder-diffraction experiments.[40,41] Except for this, our calculated value for $Li_2BeH_4$ is also comparable to the volume contraction accompanying the $\alpha \rightarrow \beta$ transition in $LiAlH_4$ (Ref. 17) and $NaAlH_4$ (Ref. 18) previously obtained, which is 17% and 4%, respectively. A large volume contraction is useful for increasing the volumetric hydrogen density of $Li_2BeH_4$ if one can find a chemical means of stabilizing the high-pressure phases. This may be possible because of the small energy difference of 283.6 meV/f.u. between the $\alpha$ and $\beta$ phases at their equilibrium volumes. Therefore, the observation of the high-pressure phase in $Li_2BeH_4$ may have technological importance. Additionally, the transformation from a monoclinic structure to an orthorhombic structure is popular for some $A_2BX_4$ compounds such as $Cs_2MoS_4$ and $Cs_2HgCl_4$ with decreasing temperatures or increasing pressures.[42,43]

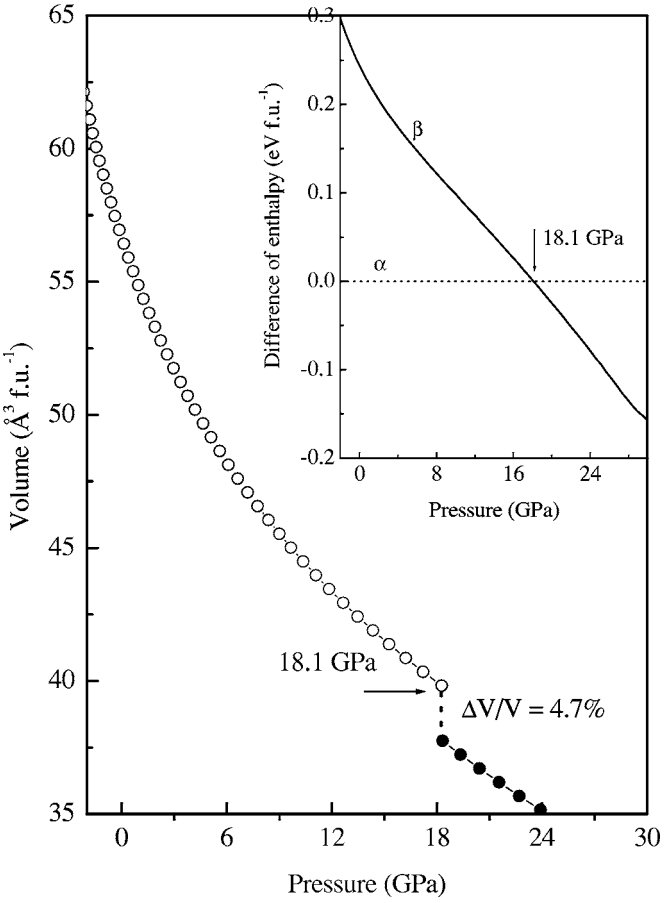


FIG. 3. Volume versus pressure curves of $\alpha$- and $\beta$-$Li_2BeH_4$. The curve of the enthalpy difference between $\alpha$- and $\beta$-$Li_2BeH_4$ versus pressure is shown in the inset.

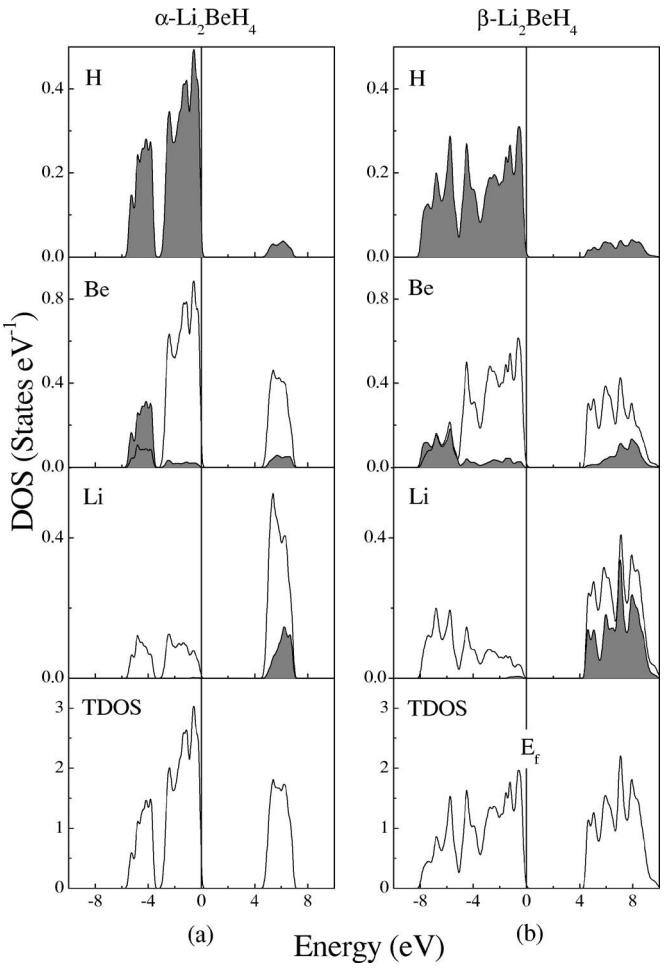


FIG. 4. Calculated total and partial electronic densities of states (DOS and PDOS) for (a) $\alpha$- (at equilibrium) and (b) $\beta$-$Li_2BeH_4$ (at transition pressure; 18.1 GPa). The Fermi level is set to zero and marked by a vertical line; *s* states are depicted as shaded-gray curves.

The calculated electronic densities of states (DOS) for $\alpha$- (at equilibrium) and $\beta$-$Li_2BeH_4$ (at transition point; 18.1 GPa) are presented in Fig. 4. From this figure, some common features can be drawn. First, $Li_2BeH_4$ exhibits a nonmetallic character with a finite energy gap ($E_g$) between the valence band (VB) and conduction band even at pressures up to 30.0 GPa, which can be considered as a representative feature of complex hydrides such as $NaAlH_4$,[18] $NaBH_4$,[19] and $Mg(AlH_4)_2$.[23] Second, in the VB region, the DOS is mainly dominated by H *s*, Be *s*,*p*, and Li *p* states and the contribution of Li *s* states is small. In addition, the Be *s*,*p* and H *s* states are energetically degenerate in the VB region. This facilitates the Be-H hybridization and thus the formation of directionally covalently bonded $BeH_4$ tetrahedron subunits in their crystal structures.

However, some marked differences can also be found from these DOS figures. First, the width of the VB is broadened from 6.05 eV in $\alpha$-$Li_2BeH_4$ to 8.52 eV in $\beta$-$Li_2BeH_4$, which is mainly due to the reduction of the interatomic distance as listed in Table II when applying pressure. Second, with the $\alpha \rightarrow \beta$ structural transition, the initial split of the VB disappears due to the hybridization of the Be *s*,*p* and H *s* states of the $BeH_4$ subunits. However, comparing with other complex hydrides such as $LiAlH_4$,[17] $NaAlH_4$,[18] and $Mg(AlH_4)_2$,[23] the decrease in the $E_g$ resulting from the volume reduction is much less. The detailed discussion of this issue will be given below.

To get a better understanding of the bonding effects between H, Be, and Li atoms, the bond overlap population (BOP) values are calculated on the basis of the Mulliken population. In general, the positive or negative BOP value indicates a bonding or an antibonding state. Here, we define a scaled BOP ($BOP^s$) as $BOP^s_{Be(Li)-H} = BOP_{Be(Li)-H}/BL_{Be(Li)-H}$; $BL_{Be(Li)-H}$ represents the average bond length of Be-H (or Li-H). The calculated BL and $BOP^s$ between H, Be, and Li atoms for $\alpha$-$Li_2BeH_4$ at ambient pressure and $\beta$-$Li_2BeH_4$ at its transition point are listed in Table II. In this table, the $BOP^s_{Be-H}$ are always positive, which can be attributed to the covalent bonding between Be and H in the $BeH_4$ subunits of $Li_2BeH_4$. On the other hand, the $BOP^s_{Li-H}$ are close to zero or negative, reflecting the ionic interactions between Li and H atoms (exactly speaking, between $Li^+$ and $[BeH_4]^-$). For a quantitative comparison of their bonding strengths with those of other metallic alanates, such as $LiAlH_4$, $NaAlH_4$, and $Mg(AlH_4)_2$, the $BOP^s$ between $M-H$ ($M$=Al, Li, Na, and Mg) for these complex hydrides

TABLE II. The average bond length (BL) and the scaled bond overlap population ($BOP^s$) between H, Li, and Be atoms in $\alpha$- (at equilibrium states) and $\beta$-$Li_2BeH_4$ (at transition points; 18.1 GPa). BL and $BOP^s$ for $LiAlH_4$, $NaAlH_4$, and $Mg(AlH_4)_2$ are given for comparison. All calculated results for their high-pressure phases are given in parentheses.

| | Be–H | | Li–H | |
|---|---|---|---|---|
| | BL | $BOP^s$ | BL | $BOP^s$ |
| $Li_2BeH_4$ | 1.425 (1.343) | 0.584 (0.718) | 1.966 (1.929) | −0.002 (−0.004) |
| | Al–H | | Li (Na, Mg)–H | |
| | BL | $BOP^s$ | BL | $BOP^s$ |
| $LiAlH_4$ | 1.620 (1.592) | 0.512 (0.521) | 2.064 (1.919) | −0.015 (−0.012) |
| $NaAlH_4$ | 1.613 (1.688) | 0.532 (0.432) | 2.427 (2.150) | −0.021 (−0.023) |
| $Mg(AlH_4)_2$ | 1.583 (1.709) | 0.483 (0.412) | 1.909 (1.953) | −0.304 (−0.148) |

are also calculated and listed in the same table. We can conclude from these results that with comparing other metallic alanates, $Li_2BeH_4$ exhibits more remarkable covalent bonding characteristic due to the stronger hybridization of the Be $s,p$ and H $s$ states resulting from the shorter bond length between Be and H atoms.

According to our aforementioned analysis and other theoretical calculations, $Li_2BeH_4$ (or other complex hydrides) can be thought of as a class of covalent compounds. Gao *et al.*[44] have pointed out that the hardness ($H_D$) of covalent crystals is closely related to the energy gap $E_g$ and the covalent bond number per unit area ($N_a$). They have deduced that $H_D = AN_aE_g$, where $A$ is a constant. Generally, the bulk modulus ($B_0$), as a measure of the resistance to compressibility of volume, is frequently used as a proxy of $H_D$, since materials with a high $B_0$ are typically very hard.[45] Hence, we could consider roughly $N_a \propto B_0/E_g$. The calculated $B_0$, $E_g$, and $B_0/E_g$ for $\alpha$- and $\beta$-$Li_2BeH_4$, $LiAlH_4$, $NaAlH_4$, and $Mg(AlH_4)_2$ are listed in Table III. It may be predicted that the larger the $N_a$ is, the stronger is the hydrogen absorption ability (or probability), but the larger the $BOP^s$ is, the lower is the hydrogen desorption ability. From this point of view, $\beta$-$Mg(AlH_4)_2$ ($B_0/E_g = 28.7$, $BOP^s = 0.412$) and $\beta$-$NaAlH_4$ ($B_0/E_g = 15.5$, $BOP^s = 0.432$) are expected to be the most promising candidates for hydrogen storage among the eight ones listed in Table III due to their good hydrogen absorption and/or desorption properties. As described in our previous work,[23] the increase in $B_0/E_g$ at the $\alpha$- to $\beta$-$Mg(AlH_4)_2$ transition at 10.3 GPa originates from an increased coordination number of Al from four to six H atoms. In contrast, the $B_0/E_g$ is increased from 6.70 to 9.39 at the $\alpha$- to $\beta$-$Li_2BeH_4$ transition at 18.1 GPa, but the $BOP^s$ raises from 0.584 to 0.718. Therefore, the improvement of the hydrogen absorption and/or desorption properties for $Li_2BeH_4$ is less significant. At this point, we must stress that for discussing the properties involved in the band gap $E_g$, the most appropriate choice is to perform the *ab initio* calculations of quasiparticle states within Hedin's *GW* approximation,[46] by which the $E_g$ in well agreement with experimental data can be obtained. However, the DFT calculations within GGA or local-density approximation (LDA) generally give rise to the well-known "band-gap problem" for semiconductors and insulators. For example, the predicted LDA band gap is typically 30%–50% (or even 100% in Ref. 47) smaller than that observed in experiments. Unfortunately, the *GW* module is still not

TABLE III. Calculated bulk modulus $B_0$ (in GPa) and energy gap $E_g$ (in eV) for $\alpha$- and $\beta$-$Li_2BeH_4$. The other theoretical values for $\alpha$- and $\beta$-$LiAlH_4$, $NaAlH_4$, and $Mg(AlH_4)_2$ are also listed for comparison. The corresponding transition pressures $P_T$ (in GPa) are given in the last column.

| | $\alpha$ (at equilibrium) | | | $\beta$ (at $P_T$) | | | |
|---|---|---|---|---|---|---|---|
| | $B_0^\alpha$ | $E_g^\alpha$ | $B_0^\alpha/E_g^\alpha$ | $B_0^\beta$ | $E_g^\beta$ | $B_0^\beta/E_g^\beta$ | $P_T$ |
| $Li_2BeH_4$[a] | 28.4 | 4.24 | 6.70 | 37.2 | 3.96 | 9.39 | 18.1 |
| $LiAlH_4$[b] | 12.9 | 4.71 | 2.74 | 25.6 | 4.25 | 6.02 | 2.7 |
| $NaAlH_4$[c] | 19.3 | 5.04 | 3.83 | 36.5 | 2.35 | 15.5 | 6.4 |
| $Mg(AlH_4)_2$[d] | 9.2 | 3.72 | 2.47 | 34.7 | 1.21 | 28.7 | 10.3 |

[a]This work.
[b]Calculated values from Ref. 17.
[c]Calculated values from Ref. 18.
[d]Calculated values from Ref. 23.

implemented in the CASTEP code and the computational cost with the *GW* approach is also expensive for large cells. The calculated *GW* band gaps for $NaAlH_4$ (Ref. 48) and $Mg(AlH_4)_2$ (Ref. 49) are 40% larger than the GGA band gaps. Accordingly, it can be assumed that the absolute values of the $E_g$ in Table III are underestimated by roughly 40% compared to the experimental finding. The relative comparison of the $E_g$ (or $B_0/E_g$) in Table III, however, would give a qualitative indication of the improvement of the hydrogen absorption and/or desorption abilities for these complex hydrides with a similar electronic structure, since their $E_g$ in this table may be underestimated to the same extent.

## IV. CONCLUSIONS

In conclusion, a detailed study on a high-pressure structural transition in $Li_2BeH_4$ has been performed by DFT. The $\alpha$-$Li_2BeH_4$ monoclinic structure observed in experiments and the other eight closely related structures with different space groups have been considered in the present work. Our calculations show that the $\alpha$-$Li_2BeH_4$ is more stable than these proposed structures at their equilibrium states and its optimized structural parameters are in well agreement with the experimental data. On application of pressure, the structural transformation from $\alpha$- to $\beta$-$Li_2BeH_4$ ($Cs_2MgH_4$ type; *Pnma*) occurs at 18.1 GPa, associated with a volume reduction of approximately 4.7%. This comes mainly from the increase in the hybridization of the Be $s,p$ with the H $s$ states in the $BeH_4$ subunits. The electronic density of states demonstrates that $\alpha$- and $\beta$-$Li_2BeH_4$ exhibit a nonmetallic character even at pressures up to 30.0 GPa. On the basis of a rough criterion of $N_a$-$BOP^s$, it would be expected that the high-pressure phases of $\beta$-$NaAlH_4$ and $\beta$-$Mg(AlH_4)_2$ are the most promising candidates among the hydrogen storage materials listed in Table III.

## ACKNOWLEDGMENT

We acknowledge the support from Grant No. 10474102 through the National Natural Science Foundation of China.

*Corresponding author. FAX: 862 42389 1320. Electronic address: ymwang@imr.ac.cn

[1] L. Schlapbach and A. Züttel, Nature (London) **414**, 353 (2001).
[2] Hydrogen Storage Challenges, Fuel Cells and Infrastructure Technologies Program-Hydrogen Storage, Energy Efficiency and Renewable Energy, U.S. Department of Energy (http://www.eere.energy.gov/hydrogenandfuelcells/storage/storage_challenges.html).
[3] B. Bogdanovic and M. Schwickardi, J. Alloys Compd. **253-254**, 1 (1997).
[4] A. Zaluska, L. Zaluski, and J. O. Ström-Olsen, J. Alloys Compd. **298**, 125 (2000).
[5] K. J. Gross, E. H. Majzoub, and S. W. Spangler, J. Alloys Compd. **356-357**, 423 (2003).
[6] S. Orimo, Y. Nakamori, G. Kitahara, K. Miwa, N. Ohba, S. Towata, and A. Züttel, J. Alloys Compd. **404-406**, 427 (2005).
[7] M. Schwarz, A. Haidue, H. Stil, P. Paulus, and H. Geerlings, J. Alloys Compd. **404-406**, 762 (2005).
[8] A. Bell and G. E. Coates, J. Chem. Soc. A **1968**, 628 (1968).
[9] J. P. Bastide, Solid State Commun. **74**, 355 (1990).
[10] B. M. Bulychev, R. V. Shapanchenko, E. V. Antipov, D. V. Sheptyakov, S. N. Bushmeleva, and A. M. Balagurov, Inorg. Chem. **43**, 6371 (2004).
[11] K. E. Lipinska-Kalita, Y. Ding, Y. Song, J. Lin, M. Somayazulu, P. Dera, J. Yarger, H. K. Mao, and R. J. Hemley, First Annual SSAAP Symposium, Albuquerque, NM, 2004 (unpublished).
[12] R. Yu and P. K. Lam, Phys. Rev. B **38**, 3576 (1988).
[13] J. L. Martins, Phys. Rev. B **38**, 12776 (1988).
[14] B. K. Rao and P. Jena, J. Phys. C **19**, 5167 (1986).
[15] M. Seel, A. B. Kunz, and S. Hill, Phys. Rev. B **39**, 7949 (1989).
[16] P. Vajeeston, P. Ravindran, A. Kjekshus, and H. Fjellvåg, Phys. Rev. Lett. **89**, 175506 (2002).
[17] P. Vajeeston, P. Ravindran, R. Vidya, H. Fjellvåg, and A. Kjekshus, Phys. Rev. B **68**, 212101 (2003).
[18] P. Vajeeston, P. Ravindran, R. Vidya, H. Fjellvåg, and A. Kjekshus, Appl. Phys. Lett. **82**, 2257 (2003).
[19] C. M. Araújo, R. Ahuja, A. V. Talyzin, and B. Sundqvist, Phys. Rev. B **72**, 054125 (2005).
[20] J. P. Bastide, B. Bonnetot, J. M. Letoffe, and P. Claudy, Mater. Res. Bull. **15**, 1215 (1980).
[21] A. V. Talyzin and B. Sundqvist, Phys. Rev. B **70**, 180101(R) (2004).
[22] M. P. Pitt, D. Blanchard, B. C. Hauback, H. Fjellvåg, and W. G. Marshall, Phys. Rev. B **72**, 214113 (2005).
[23] C. H. Hu, D. M. Chen, Y. M. Wang, D. S. Xu, and K. Yang, J. Phys.: Condens. Matter **19**, 176205 (2007).
[24] J. P. Perdew, J. A. Chevary, S. H. Vosko, K. A. Jackson, M. R. Pederson, D. J. Singh, and C. Fiolhais, Phys. Rev. B **46**, 6671 (1992).
[25] M. D. Segall, P. L. D. Lindan, M. J. Probert, C. J. Pickard, P. J. Hasnip, S. J. Clark, and M. C. Payne, J. Phys.: Condens. Matter **14**, 2717 (2002).
[26] T. H. Fischer and J. Almlof, J. Phys. Chem. **96**, 9768 (1992).
[27] G. Kresse and J. Furthmuller, Phys. Rev. B **54**, 11169 (1996).
[28] B. Bertheville, P. Fischer, and K. Yvon, J. Alloys Compd. **302**, L12 (2000).
[29] P. Seiler, Acta Crystallogr., Sect. B: Struct. Sci. **14**, 223 (1993).
[30] W. Eysel, H. H. Höfer, K. L. Keester, and Th. Hahn, Acta Crystallogr., Sect. B: Struct. Sci. **41**, 5 (1985).
[31] A. S. Koster, F. X. N. M. Kools, and G. D. Rieck, Acta Crystallogr., Sect. B: Struct. Crystallogr. Cryst. Chem. **25**, 1704 (1969).
[32] P. M. Skarstad and S. Geller, Mater. Res. Bull. **10**, 791 (1975).
[33] F. S. Galasso, *Structure and Properties of Inorganic Solids* (Pergamon, New York, 1970).
[34] J. Fabry, T. Breczewski, F. J. Zuniga, and A. R. Arnaiz, Acta Crystallogr., Sect. C: Cryst. Struct. Commun. **49**, 946 (1993).
[35] P. Vinet, J. H. Rose, J. Ferrante, and J. R. Smith, J. Phys.: Condens. Matter **1**, 1941 (1989).
[36] F. D. Murnaghan, Proc. Natl. Acad. Sci. U.S.A. **30**, 8244 (1944).
[37] F. Birch, Phys. Rev. **71**, 809 (1947).

[38] D. Setoyama, J. Matsunaga, H. Muta, M. Uno, and S. Yamanaka, J. Alloys Compd. **381**, 215 (2004).
[39] K. Tatsumi, I. Tanaka, K. Tanaka, H. Inui, M. Yamaguchi, H. Adachi, and M. Mizuno, J. Phys.: Condens. Matter **15**, 6549 (2003).
[40] J. D. Jorgensen, Z. Hu, S. Teslic, D. N. Argyriou, S. Short, J. S. O. Evans, and A. W. Sleight, Phys. Rev. B **59**, 215 (1999).
[41] S. Carlson and Annie Marie Krogh Andersen, Phys. Rev. B **61**, 11209 (2000).
[42] B. Lorenz, I. Orgzall, P. K. Dorhout, C. C. Raymond, K. Brister, K. Weishaupt, R. D'Adamo, and H. D. Hochheimer, Phys. Rev. B **55**, 2800 (1997).
[43] B. Bagautdinov, A. Jobst, J. Ludecke, and S. van Smaalen, Acta Crystallogr., Sect. B: Struct. Sci. **57**, 231 (2001).
[44] F. M. Gao, J. L. He, E. D. Wu, S. M. Liu, D. L. Yu, D. C. Li, S. Y. Zhang, and Y. J. Tian, Phys. Rev. Lett. **91**, 015502 (2003).
[45] M. L. Cohen, Solid State Commun. **92**, 45 (1994).
[46] L. Hedin, Phys. Rev. **139**, A796 (1965).
[47] W. D. Luo, S. Ismail-Beigi, M. L. Cohen, and S. G. Louie, Phys. Rev. B **66**, 195215 (2002).
[48] A. Peles, J. A. Alford, Z. Ma, L. Yang, and M. Y. Chou, Phys. Rev. B **70**, 165105 (2004).
[49] M. J. van Setten, G. A. de Wijs, V. A. Popa, and G. Brocks, Phys. Rev. B **72**, 073107 (2005).